www.dergipark.gov.tr
ISSN:2148-3736

El-Cezerî Journal of Science and Engineering
Vol: 10, No: 2, 2023 (305-325)
DOI: 10.31202/ecjse.1213826

ECJSE

Research Paper

K^+ Channels and Some Familiar Antiepileptic Drugs: Evaluation of Their the Structure-Activity Relationships with Molecular Docking Analysis

Esra Nur ÇAKMAK[1a*], Mahmut GÜR[2b], Bayram KIRAN[3c]

[1]Genetics and Bioengineering of Department, Kastamonu University, Kastomonu, Kastamonu, Turkey,
[2]Forest Industrial Engineering of Department, Kastamonu University, Kastamonu, Turkey,
[3]Genetics and Bioengineering of Department, Kastamonu University, Kastomonu, Turkey,
kmrc_1675@hotmail.com

Received/Geliş: 02.12.2022 **Accepted/Kabul:** 17.04.2023

Abstract: This study includes the structure-activity relationship of active molecules that are commonly used in the treatment of convulsive seizures in epileptic diseases. Well-known epileptic active molecules studied are: Vigabatrin, Lokosamidine, Zonisamide, Oxcarbazepine, Levetiresetam, Tiagabine, Topiramate, Lamotrigin, Gabapentin, Felbamat, Ethosuximide, Valproic Acid, Mesuximide, Ethotoin, Primidon, Trimethadion, Phenytoin, Remasemide, Mephenytoin. These molecules, which were selected considering the physiopathological mechanisms of action of epileptic disease, were considered suitable for molecular docking studies since they were used as a potential antiepileptic agent. In addition, it was focused on the potassium channels, which were prominent in the mechanisms of epilepsy. During the action potential that triggers seizure formation, inward rectifying potassium channels (KIR3.2) make a important role providing the flow of K^+ ions. Thus, PDB ID: 4KFM receptor was chosen for molecular docking study, since its act as an agonist according to its activity on the canal in the case of epileptic seizures formation. The result of molecular docking analysis demonstrated that Phenytoin gave the best binding affinity for 4KFM with a value of -6.2 kcal/mol. Other analysis in descending order (as kcal/mol); Oxcarbazepine (-6,0), Remasemide (-5.9), Topiramate and Primidon (-5.8), Tiagabine, Felbamat and Mesuximide (-5.7), Lamotrigin (-5.6) Zonisamide, Ethotoin and Mephenytoin, Lokosamidine (-5.5), Gabapentin (-4.8), Trimethadion (-4.7), Ethosuximide (-4.6), Levetiresetam (-4.5), Vigabatrin (-4.0), Valproic Acid (-3.9) determined as.

Keywords: Antiepileptic, Drug, Moleculer Docking, Potassium channel, Epilepsy

1. Introduction

Epilepsy is a central nervous system disease that affects 1-2% of the world population and is characterized by the disruption of the balance between excitatory and inhibitory voltage-dependent/synaptic transmission and excessive shaking of the body as a result of structural or functional changes in the brain [1,2]. These changes can lead to the development of epilepsy in a particular region of the brain, with the occurrence of functional disorders in macromolecules involved in excitatory and inhibitory transmission in an epileptic brain [3]. GABA is the main inhibitor of neuronal excitability in the brain, and it does this through the GABA-A and GABA-B receptors [4]. The binding of GABA to the GABA-B receptor increases the potassium current, decreases calcium ion input, and inhibits the presynaptic release of other neurotransmitters [5].

Genetic, molecular, physiological, and pharmacological findings are known that Kir3.2, a subunit of potassium channels, plays a role in the control of epileptogenesis and neuronal excitability. The main task of Kir channels is to control cell excitability by converting action potential to membrane resting potential. Kir channels carrying K^+ ions into the cell to bring the cell hyperpolarized at the end of the action potential to its normal resting potential accelerate repolarization, making the action potential a repeatable process. Active Kir channels play a key role in activation by stimulating the cell by causing

How to cite this article
Çakmak E. N., Gür M., Kıran B., "K+ Channels and Some Familiar Antiepileptic Drugs: Evaluation of Their the Structure-Activity Relationships with Molecular Docking Analysis," *El-Cezerî Journal of Science and Engineering*, Vol. 10, No. 1, pp. 305-325, 2023.
ORCID: [a]0000-0003-4033-5190; [b]0000-0001-9942-6324; [c]0000-0001-9796-6028

membrane hyperpolarization [6,7]; while the increase in the function of the channels reduces neuronal activity, loss of their functions leads to excessive neuronal stimulation and epilepsy [8]. This stuation shows that potassium channels will be potential targets of new AEDs [9] and advances in drug screening technology have been instrumental in considering potassium channel agonists as AEDs [10]. On the other hand, antiepileptic drugs used in the treatment of epilepsy can be categorized based on act the potassium channel in various different mechanisms. In a study conducted by Doupnik in the literature in 2019, Kir channels targeted by the venom peptide tertiapin (TPN) were emphasized. In the molecular docking study with 4KFM, it was observed that the TPN-13 structure gave the highest affinity value for Kir3.2 channel [11]. In another study, Zhao (2020) et al, examined the G-protein-gated inward K^+ channel (GIRK) of the 4KFM macromolecule, and pharmacologically targeting subsets of GIRK channels that may provide new opportunities to improve the treatment of neurological disorders stemmed from various therapeutic effects in the brain [12]. For similar reasons in the mentioned studies, 4KFM macromolecule was chosen considering the above-mentioned conditions, in this study.

In the study, Vigabatrin, Lokosamidine, Zonisamide, Oxcarbazepine, Levetiresetam, Tiagabine, Topiramate, Lamotrigine, Gabapentin, Felbamate, Ethosuximide, Valproic Acid, Mesuximide, Ethotoin, Primidone, Trimethadion, Phenytoin, Remasemide, Mephenytoin were used as ligand. And these ligands are embedded in the 4KFM protein.

The molecular interaction bond structures and properties obtained from the newly created ligand-4KFM structure were examined. The Autodock Vina program and Discovery Studio programs mentioned in the following sections were used for these placement processes. The obtained data are presented in 2D and 3D.

2. Experimental Methods

2.1. Materials

PDB ID: 4KFM macromolecule obtained from RCSB PDB database is a macromolecule studied on the crystal structure of the inward rectifier K^+ channel GIRK2 (Kir3.2) gated in complex with β- ץ G protein subunits [13]. This macromolecule was chosen from among the molecules that produce agonist effects for the ion-gated potassium channel. Considering that potassium channels have an inhibitory effect in the formation of seizures and it is known that the channel Kir3.2 in the infrastructure of the potassium channel plays an active role in the treatment of epilepsy, the 4KFM structure has been chosen as a macromolecule suitable for the action mechanism of the ligands [14].

The nomenclatures, molecular structures, and mechanisms of action of the AED active ingredients used in this study are presented in Table 1: Vigabatrin, Lokosamidine, Zonisamide, Oxcarbazepine, Levetiresetam, Tiagabine, Topiramate, Lamotrigine, Gabapentin, Felbamat, Ethosuximide, Valproic Acid, Mesuximide, Ethotoin, Primidon, Trimethadion, Phenytoin, Remasemide, Mephenytoin and their 3D structures are accessed from PubChem database.

2.2. Method

Molecular docking analysis was applied to determine the interactions between the active ingredients determined according to their high potential on ion channels for the treatment of epilepsy and the protein targeting their mechanisms and to calculate the binding energy. In the study carried out with this method, firstly, the structures previously studied were extracted from the receptor structure in the Discovery Studio 2020 Client [15] and the ligand structures were recorded in .pdb format. In the second step, the structures saved in .pdb format were converted to .pdbqt format by following the necessary steps in the Autodock Vina program [16,17], which is the Autodock Tools interface. Then,

the conformational structure with the best binding affinity was sent into the receptor and the interactions were examined.

Table 1. The nomenclatures, molecular structures and mechanisms of action of the aed active ingredients

Names	Mechanisms of Action	Chemical Structures
Ethotoin	Na^+ channel inhibition	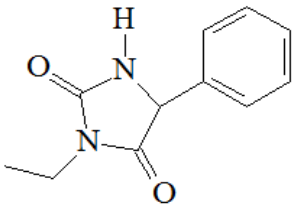
Ethosüksimide	T-type Calcium (Ca^{2+}) channel inhibition	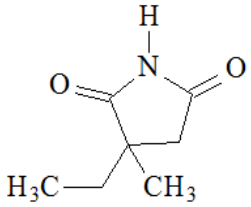
Felbamat	Glutamate inhibition, NMDA receptor blockage, increases GABA levels, Na^+ channel blockade, blockade of voltage-gated Ca^{2+} channels	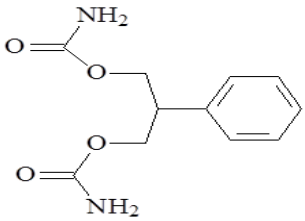
Gabapentin	Increases GABA levels, Calcium channel modification	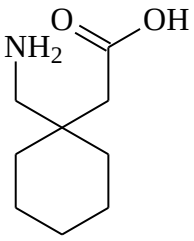
Lamotrigine	Voltage-gated sodium channel inhibition, glutamate reduction, Ca^{2+} channel inhibition	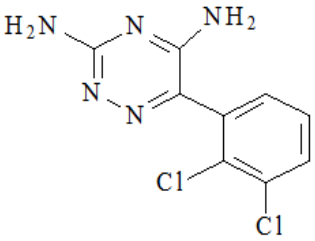
Levetirasetam	Modulation of synaptic vesicle proteins, N, T-type Ca^{2+} Channel inhibition, increases voltage-gated potassium channel conductivity, increases GABA concentration, and inhibits glutamate system by stimulating	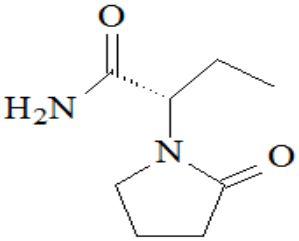

Fenitoine	Sodium and calcium channel inhibition activates K^+ channel transmission, increases GABA concentration	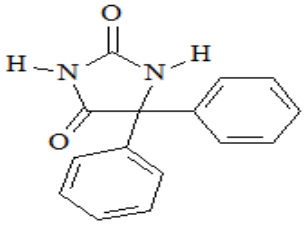
Primidon	GABA increase, Glutamate decrease, Na^+, Ca^{2+} channel inhibition, K+ channel opening	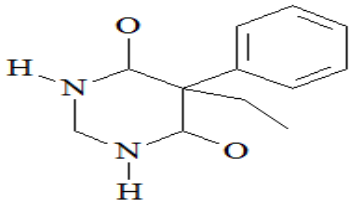
Oxcarbazepine	Sodium channel inhibition, N, P, R type Ca^{2+} channel inhibition	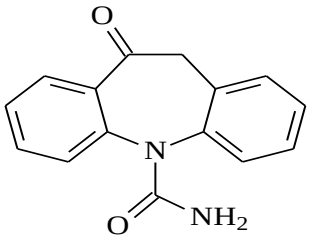
Tiagabine	Increases GABA concentrations and inhibits GABA-AT	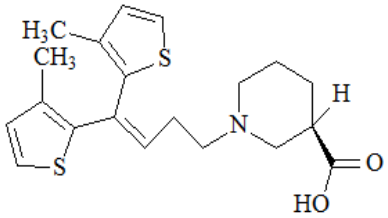
Topiramat	Glutamate reduction, voltage-transition sodium channel inhibition, activation of potassium currents, AMPA and glutamate inhibition, voltage-transition calcium channel inhibition, NMDA inhibition, increase of GABA concentration, inhibition of carbonicanhydrase isoenzyme	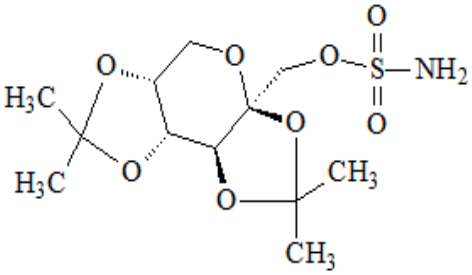
Valproic acid	Na^+ and T type Ca^{2+} channel inhibition, GABA increase, K^+ channel activity	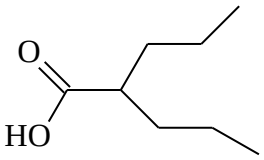
Vigabatrin	GABA increase opens K^+ (potassium) channels, increases Cl^- channel opening, GABA-AT inhibition effect	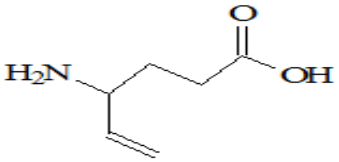
Zonisamide	T-type Calcium channel inhibition, Inhibit Carbonic Anhydrase isoenzyme, voltage-gated Na^+ channel inhibition, inhibit glutamate release	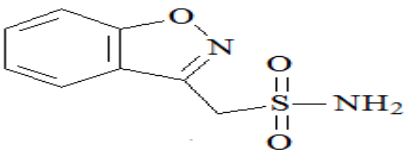

Lakosamide	It increases the slow inactivation phase of the Na^+ channel and is responsible for blocking the voltage-gated sodium channel.	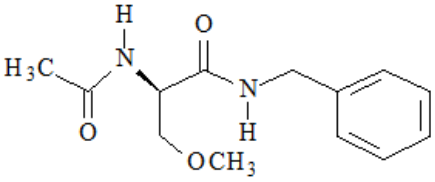
Mesuximide	T-type Ca^{2+} channel inhibition, partial NMDA inhibition	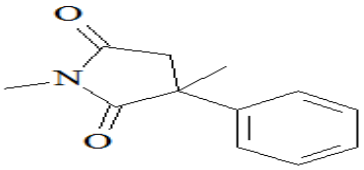
Trimethadione	T-type Ca^{2+}, Na^+ channel inhibition, partial NMDA inhibition	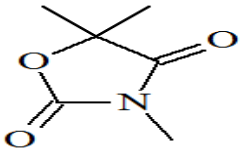
Mephenytoine	Inhibits voltage-gated Na^+ channel conduction	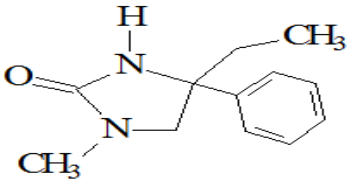
Remasemide	Blocks NMDA responses, inhibits voltage-gated Na^+ channel conduction	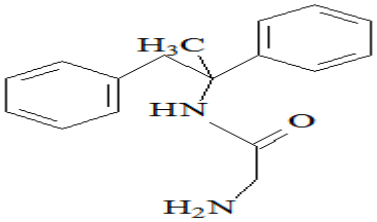

2.3. Molecular Docking Analysis

4KFM macromolecule is selected according to the mechanism of agonist effect in terms of potassium channel for neurotransmitters in epilepsy, and consists of three chains consisting of A, B, G. For the coupling process of the 4KFM macromolecule in this study, the A chain with active binding sites in all ligands was randomly selected. The following amino acid active sites have been determined for the binding sites; LYS 90, TRP 91, ARG 92, LYS 194, LYS 199, LYS 200. Research area is 375Å interval value, grid size is determined as 48Å × 44Å × 46Å for all ligands. The location of this research area was set for all ligands, the X, Y and Z coordinates of the center to -54.479, -47.165 and -62.864 and each recorded in the conf.txt file. The vina.exe file prepared by The Scripps Research Institute, which enables the Vina program to run before the docking phase begins, was called through the script system, after that, the folder containing the conf.txt file to be used in the docking phase was called. Then the program was run and out.pdbqt file containing 10 conformation was created. The equation used to find the best binding energy is as follows;

$$\Delta G = \Delta GvdW + \Delta GHbond + \Delta Gelec4\Delta Gto + \Delta Gdesolv \quad (1)$$

ΔG: represents a change in energy.

3. Results and Discussion

In the Discovery Studio 2020 Client program, the conformation that gives the best value was placed

inside the 4KFM macromolecule to see 2D and 3D structures. The binding affinity values obtained for ligands as a result of this calculation are summarized in Table 2.

Table 2. The binding affinity values of ligands placed in 4KFM at the best conformation

Ligand's	Best Binding affinity (kcal/mol)	Distance from best mode (Å)	
		RMSD l.b	RMSD u.b
Vigabatrin	-4,0	0,000	0,000
Locosamidine	-5,0	0,000	0,000
Zonisamide	-5,5	0,000	0,000
Oxcarbazepine	-6,0	0,000	0,000
Levetiracetam	-4,5	0,000	0,000
Tiagabine	-5,7	0,000	0,000
Topiramate	-5,8	0,000	0,000
Lamotrigine	-5,6	0,000	0,000
Gabapentin	-4,8	0,000	0,000
Felbamate	-5,7	0,000	0,000
Ethosuximide	-4,6	0,000	0,000
Valproic Acid	-3,9	0,000	0,000
Mesuximide	-5,7	0,000	0,000
Ethotoin	-5,5	0,000	0,000
Primidone	-5,8	0,000	0,000
Trimethadione	-4,7	0,000	0,000
Phenytoin	-6,2	0,000	0,000
Remasemide	-5,9	0,000	0,000
Mephenytoine	-5,5	0,000	0,000

3.1. Vigabatrin

The affinity value of vigabatrin placed in the macromolecule 4KFM in the best binding mode was obtained as -4.0 kcal/mol and 2D and 3D pictures of the intermolecular interactions between vigabatrin and macromolecule 4KFM are given in Fig. 1.

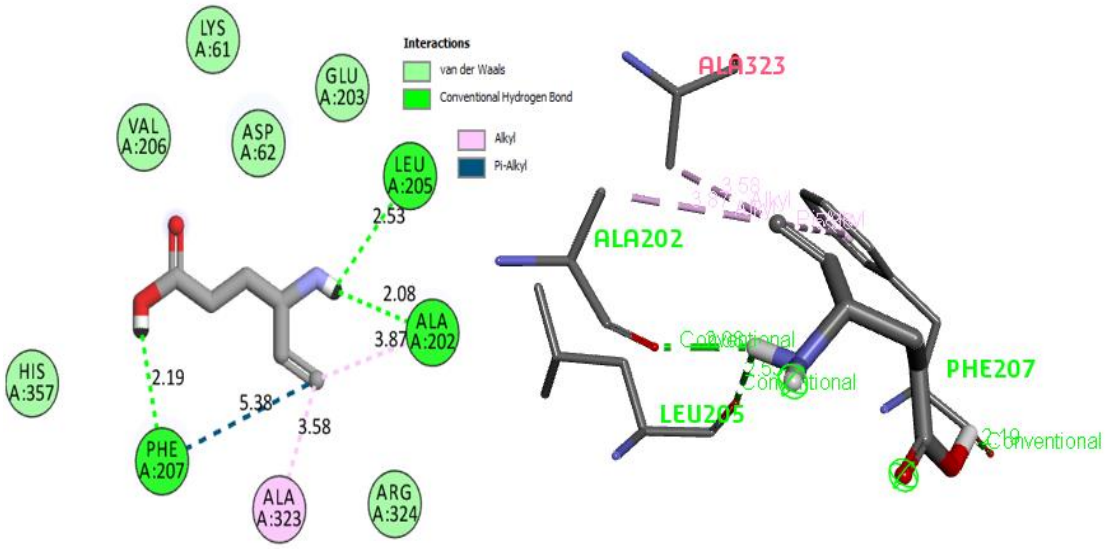

Figure 1. 2D and 3D representation of vigabatrin and 4KFM macromolecule.

The resulting ligand-protein interactions are as follows; PHE_A202, ALA_A323 and ALA_A202 amino acid binding sites 5.38Å, 3.58Å and 3.87Å, respectively, with a double bonded oxygen atom; pi-

alkyl formed the interaction with alkyl and alkyl bond lengths. The PHE_A207 amino acid binding site forms a conventional 2.19Å long hydrogen bond interaction with the hydroxyl group; the amino acid active sites ALA_A202 and TYR_A205 formed the conventional hydrogen bond interaction with the amine at repeat lengths of 2.08A and 2.53A, respectively (Table 3).

3.2. Lamotrigine

The affinity value of lamotrigine was obtained as -5.6 kcal/mol and the intermolecular interaction patterns are presented in the fig. 2. Interactions are as follows; ARG_A230, LYS_A200, ARG_A231 and VAL_A314 amino acid active sites 4,12Å with benzene group; 4.69Å; More pi-cations, pi-alkyl, pi-alkyl and pi-sigma bond interference of 5.32Å and 3.99Å length; the amino acid active sites of VAL_A314 and ALA_B316 formed the methyl group with an alkyl bond of 5.25Å and 4.15Å length (Table 3).

Table 3. Interactions, types and distances between vigabatrin and lamotrigine and 4KFM macromolecule

Vigabatrin				Lamotrigine			
Residue	**Ligand group**	**Distance (Å)**	**Interaction**	**Residue**	**Ligand group**	**Distance (Å)**	**Interaction**
PHE_A207	O atom in vigabatrin	5,38	Pi- Alkyl	ARG_A230	Benzene group in Lamotrigine	4,12	Pi-Cation
ALA_A323	O atom in vigabatrin	3,58	Alkyl	LYS_A200	Benzene group in Lamotrigine	4,69	Pi-Alkyl
ALA_A202	O atom in vigabatrin	3,87	Alkyl	ARG_A231	Benzene group in Lamotrigine	5,32	Pi-Alkyl
PHE_A207	OH compound in vigabatrin	2,19	Conventional hydrogen bond	VAL_A314	Benzene group in Lamotrigine	3,99	Pi-Sigma
ALA_A202	NH_2 compound in vigabatrin	2,08	Conventional hydrogen bond	VAL_A314	CH_3 compound in Lamotrigine	5,25	Alkyl
LEU_A205	NH_2 compound in vigabatrin	2,53	Conventional hydrogen bond	ALA_B316	CH_3 compound in Lamotrigine	4,15	Alkyl

The interactions found for vigabatrin and lamotrigine are shown in table 3.

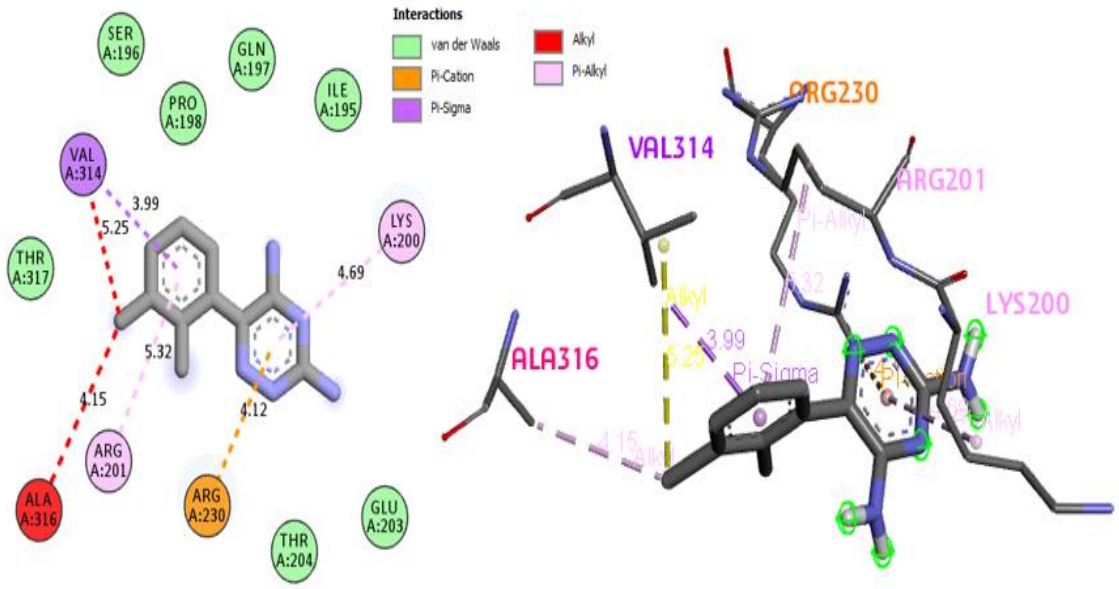

Figure 2. 2D and 3D representation of lamotragine and 4KFM macromolecule

3.3. Ethosuximide

Molecular interactions between the ligand with affinity value given as -4.6 kcal/mol and the macromolecule 4KFM are shown in the fig. 3 and the interactions are the; 2,12Å long hydrogen bond interaction with GLN_A322 amino acid active site amine group; LYS_A64 amino acid active site methyl group 4.72Å long alkyl bond interaction; LYS_A199 and ALA_B202 amino acid active sites formed 3,34Å and 4,15Å long alkyl bond interactions with the methylene group (Table 4).

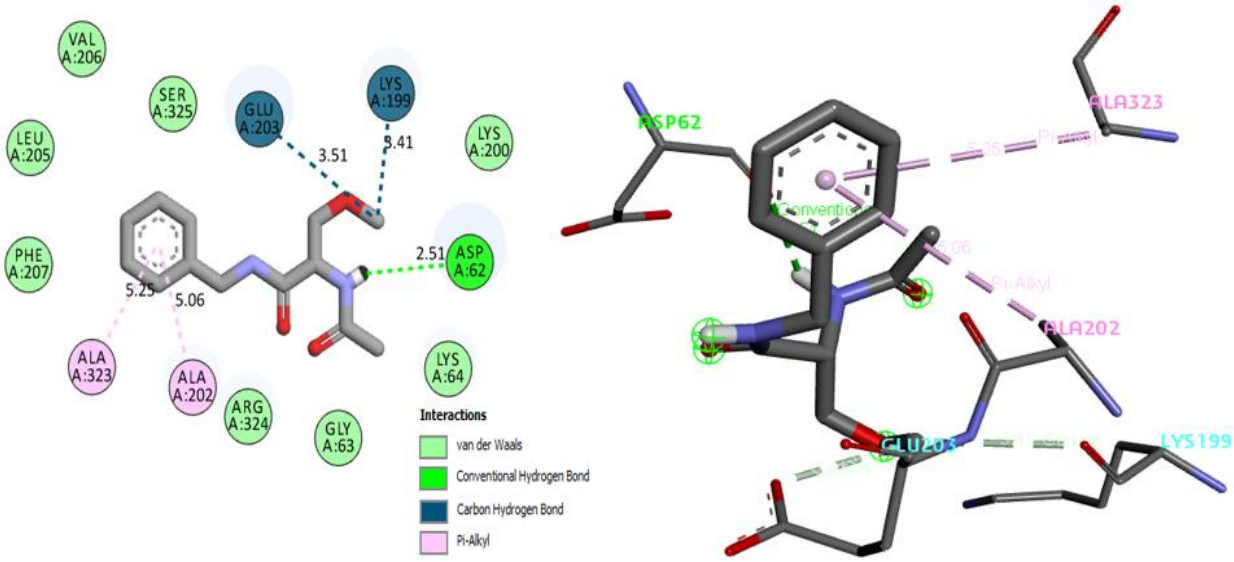

Figure 3. 2D and 3D representation of ethosuximid and 4KFM macromolecule

3.4. Locosamidine

Molecular interactions between locosamide and 4KFM with affinity values of -5.0 kcal/mol are shown in the fig. 4. Interactions; conventional hydrogen bond interaction with the amine of the ASP_A62 amino acid active site at a distance of 2.51Å; carbon-hydrogen bond interaction with carbon monoxide at the amino acid regions of GLU_A203 and LYS_A199 at 3.51Å and 3.41Å, respectively; ALA_A323 and ALA_A202 amino acid binding sites formed a pi-alkyl bond interaction with benzene group of 5.25Å and 5.06Å length, respectively (Table 4).

Table 4. Interactions, types and distances between ethosuximide and lokosamidine and 4KFM macromolecule

Ethosuximide				Locosamide			
Residue	**Ligand group**	**Distance (Å)**	**Interaction**	**Residue**	**Ligand group**	**Distance (Å)**	**Interaction**
GLN_A322	NH_2 compound in ethosuximide	2,12	Conventional hydrogen bond	ASP_A62	NH_2 compound in locosamide	2,51	Conventional hydrogen bond
LYS_A199	CH_2 compound in ethosuximide	3,24	Alkyl	GLU_A203	CO compound in locosamide	3,51	Carbon hydrogen bond
ALA_B202	CH_2 compound in ethosuximide	4,15	Alkyl	LYS_A199	CO compound in locosamide	3,41	Carbon hydrogen bond
LYS_A64	CH_3 compound in ethosuximide	4,72	Alkyl	ALA_A323	Benzene group in locosamide	5,25	Pi-alkyl
GLN_A322	NH_2 compound in ethosuximide	2,12	Conventional hydrogen bond	ALA_A202	Benzene group in locosamide	5,06	Pi-alkyl

The interactions found for ethosuximide and locosamide are shown in Table 4.

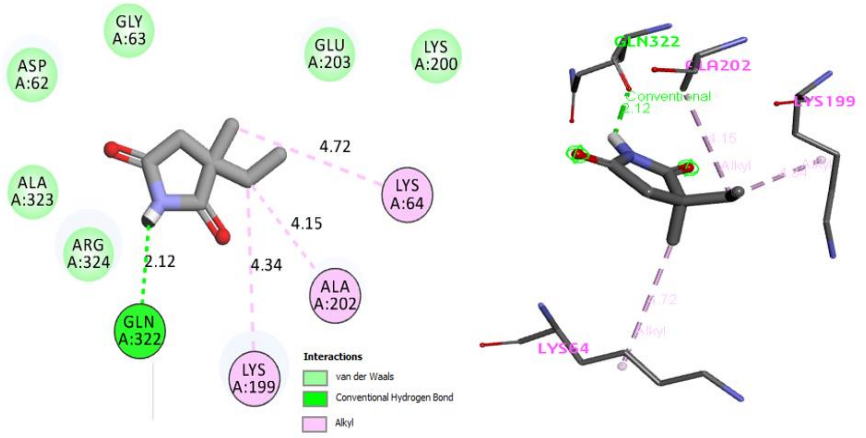

Figure 4. 2D and 3D representation of lacosamide and 4KFM macromolecule

3.5. Zonisamide

The affinity value of the ligand zonisamide placed in 4KFM at the best binding position was obtained as -5.5 kcal/mol and the interactions between the best binding mode of zonisamide and 4KFM are shown as fig. 5. The obtained ligand-protein interactions are the; conventional hydrogen bond interaction with GLN_A197 and ILE_A195 amino acid binding sites at 2.84A19 and 2.94Å distance, respectively; 3.72Å long carbon bond interaction with ARG_A201 amino acid active site nitrogen atom; the amino acid binding sites ARG_A230, ARG_A201 and LYS_A200 with benzoxaline group were pi-cation, pi-alkyl and pi-alkyl bond interaction at 4,10Å; 5,08Å and 5,01Å lengths, respectively. The ARG_A200 amino acid active site formed a 4.01Å long pi-alkyl bond interaction with the benzene group (Table 5).

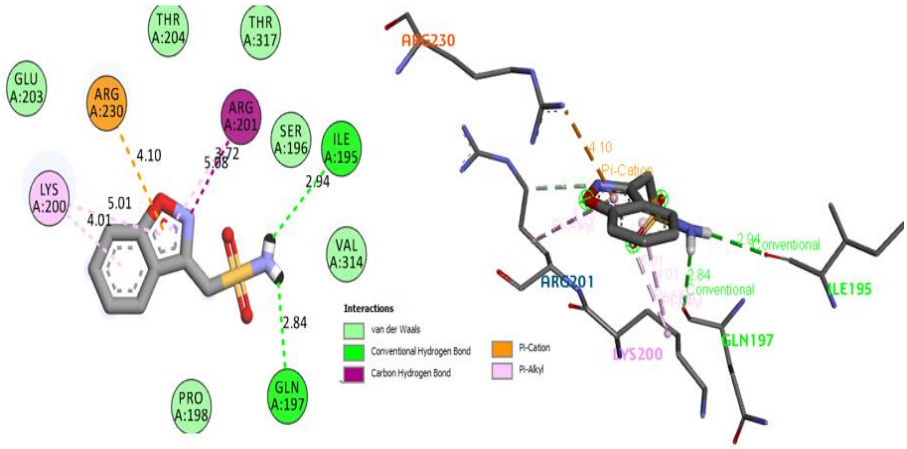

Figure 5. 2D and 3D representation of zonisamide and 4KFM macromolecule

3.6. Felbamate

The patterns of the interactions between the felbamate best binding position and 4KFM with an affinity value of -5.7 kcal/mol are shown in the fig. 6 and the molecular coupling interactions obtained are as follows; the amino acid active sites ALA_A202, ALA_A203, LEU_A205 and LEU_A205 with the amine group were respectively 2.80Å; 2.00Å; conventional hydrogen bond interaction of 2.31Å and 2.00Å length; 4.94Å long pi-alkyl bond interaction with benzene group of LYS_A61 amino acid active site; 3.76Å long carbon hydrogen bond interaction with the methylene group of the LEU_A205 amino

acid active site; the GLU_A203 amino acid active site formed a 3,44Å-long carbon-hydrogen bond interaction with the O atom (Table 5).

Table 5. Interactions, types and distances between zonisamide and felbamate and the 4KFM macromolecule

Zonisamide				Felbamat			
Residue	**Ligand group**	**Distance (Å)**	**Interaction**	**Residue**	**Ligand group**	**Distance (Å)**	**Interaction**
GLN_A197	NH_2 compound in zonisamide	2,84	Conventional hydrogen bond	ALA_A202	NH_2 compound in felbamate	2,80	Conventional hydrogen bond
ILE_A195	NH_2 compound in zonisamide	2,94	Conventional hydrogen bond	GLU_A203	NH_2 compound in felbamate	2,00	Conventional hydrogen bond
ARG_A201	Nitrogen atom in zonisamide	3,72	Carbon hydrogen bond	GLU_A203	O atom in felbamate	3,44	Carbon hydrogen bond
ARG_A230	Benzaxazoline group in zonisamide	4,10	Pi-Catiın	LEU_A205	NH_2 compound in felbamate	2,31	Conventional hydrogen bond
ARG_A201	Benzaxazoline group in zonisamide	5,08	Pi-Alkyl	LEU_A205	NH2 compound in felbamate	2,00	Conventional hydrogen bond
LYS_A200	Benzaxazoline group in zonisamide	5,01	Pi-Alkyl	LEU_A205	The methylene group in felbamate	3,76	Carbon hydrogen bond
LYS_A200	Benzene group in zonisamide	4,01	Pi-Alkyl	LYS_A61	The benzene group in felbamate	4,94	Pi- Alkyl

The interactions found for zonisamide and felbamat are shown in table 5.

3.7. Oxcarbazepine

The binding affinity value of the ligand oxcarbazepine placed in the macromolecule 4KFM at the best binding position was obtained as -6.6 kcal / mol. 2D and 3D visualizations of intermolecular interactions between the position in the best binding mode of oxcarbazepine and 4KFM are provided in the fig. 7. The resulting ligand-protein interactions were the; ALA_A202 and ALA_A323 amino acid active sites formed 4.95Å and 5.34Å long pi-alkyl bond interactions with benzene group (Table 6).

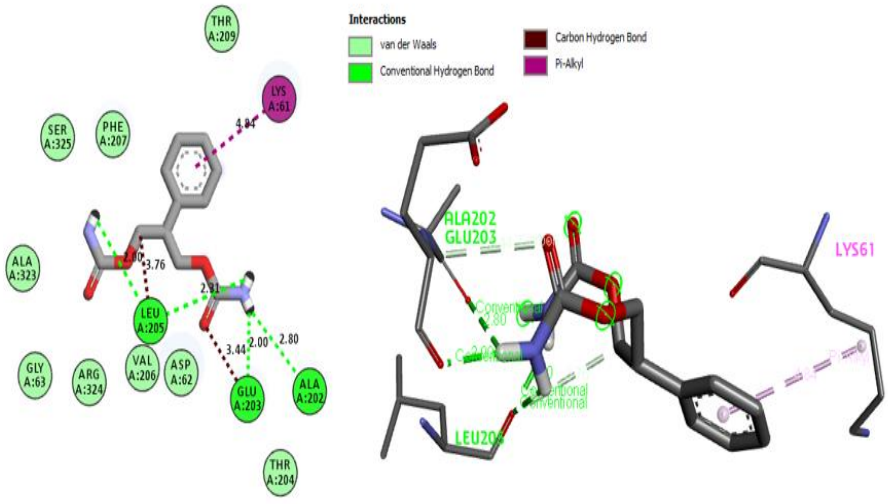

Figure 6. 2D and 3D representation of felbamat and 4KFM macromolecule

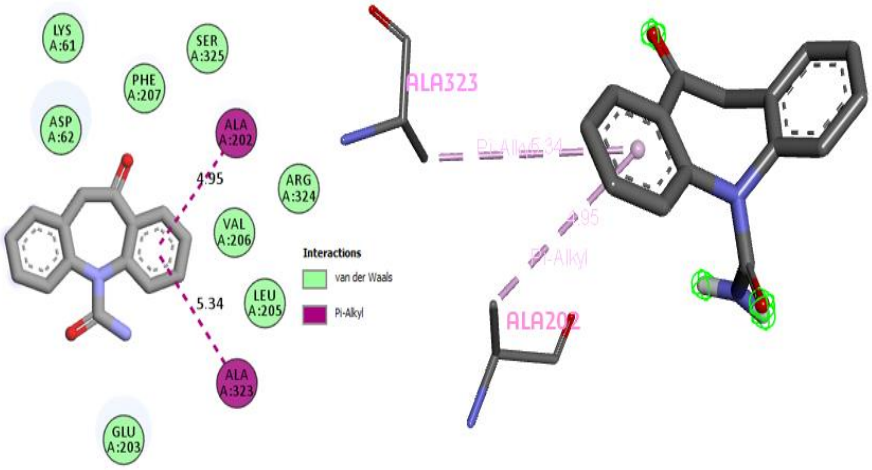

Figure 7. 2D and 3D representation of oxcarbazepine and 4KFM macromolecule

Table 6. Interactions, types and distances between oxcarbazepine and tiagabine and 4KFM macromolecule

Oxcarbazepine				Tiagabine			
Residue	**Ligand group**	**Distance (Å)**	**Interaction**	**Residue**	**Ligand group**	**Distance (Å)**	**Interaction**
ALA_A202	Benzene group in oxcarbazepine	4,95	Pi-Alkyl	LYS_A61	Benzene group in tiagabine	4,16	Alkyl
ALA_A323	Benzene group in oxcarbazepine	5,34	Pi-Alkyl	VAL_A206	CH_3 compound in tiagabine	4,84	Alkyl

The interactions found for oxcarbazepine and tiagabine are shown in table 6.

3.8. Tiagabin

The binding affinity value of tiagabine was obtained as -5.7 kcal/mol, and the links between the best binding mode and 4KFM are shown in the fig. 8. The ligand-protein communications obtained are the; LYS_A61 amino acid binding site with benzene group at 4.16Å distance alkyl bond interaction; the VAL_A206 amino acid active site formed a 4.84Å long alkyl bond interaction with the methylene group (Table 6).

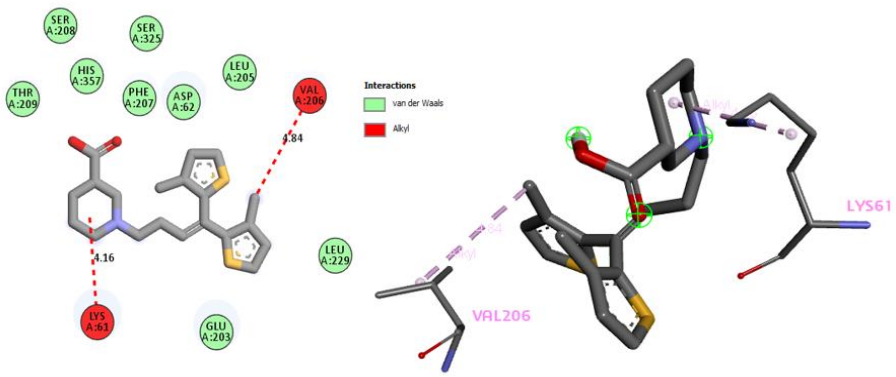

Figure 8. 2D and 3D representation of tiagabin and 4KFM macromolecule

3.9. Gabapentin

The affinity value of gabapentin at the best binding position was obtained as -4.8 kcal/mol, and the patterns of interactions between gabapentin and 4KFM are shown in the fig. 9. Interactions after molecular coupling study are the; GLU_A203, GLU_A203 and LEU_A205 amino acid active sites with amine compound respectively 2.47A ile; they formed the conventional hydrogen bond interaction of 2.90Å and 2.20Å in length (Table 7).

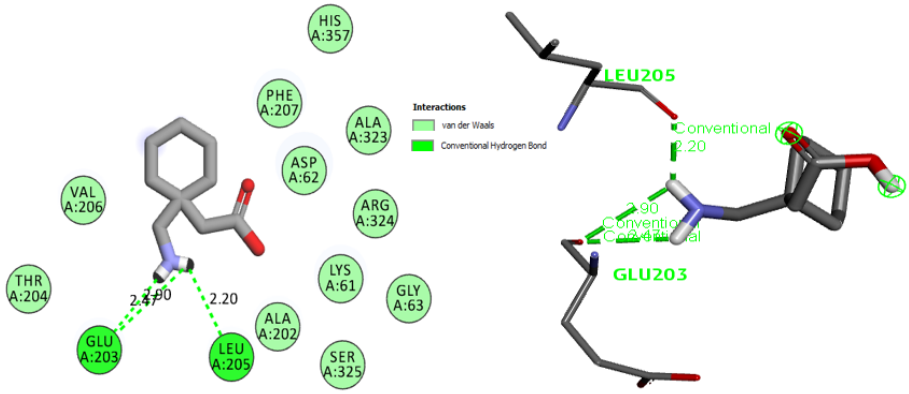

Figure 9. 2D and 3D representation of gabapentin and 4KFM macromolecule

3.10. Valproic Acid

The affinity value of valproic acid placed in 4KFM at the best binding position was obtained as -3.9 kcal/mol, and pictures of the molecular interactions between valproic acid and 4KFM are given in the fig. 10. Interactions after the study are as follows; conventional hydrogen bonding interaction of LEU_A205 and ALA_A202 amino acid active sites with hydrogen atom with lengths of 2.00Å and 2.39Å, respectively; PHE_A207 amino acid active site formed a 5.30Å long pi-alkyl bond interaction with the methylene group (Table 7).

Table 7. Interactions, types and distances between gabapentin and valproic acid and 4KFM macromolecule

Gabapentin				Valproic Acid			
Residue	**Ligand group**	**Distance (Å)**	**Interaction**	**Residue**	**Ligand group**	**Distance (Å)**	**Interaction**
GLU_A203	NH_2 compound in gabapentin	2,47	Carbon hydrogen bond	LEU_A205	Hydrogen atom in valproic acid	2,00	Carbon hydrogen bond
GLU_B155	NH_2 compound in gabapentin	2,90	Carbon hydrogen bond	ALA_A202	Hydrogen atom in valproic acid	2,39	Carbon hydrogen bond
LEU_A205	NH_2 compound in gabapentin	2,20	Carbon hydrogen bond	PHE_A207	CH_2 group in valproic acid	5,30	Pi-Alkyl

The interactions found for gabapentin and valproic acid are shown in Table 7.

3.11. Primidon

The affinity value of primidone placed in 4KFM at the best binding position was obtained as -5.8 kcal/mol and the molecule interactions between primidone and macromolecule are given in the fig. 11.

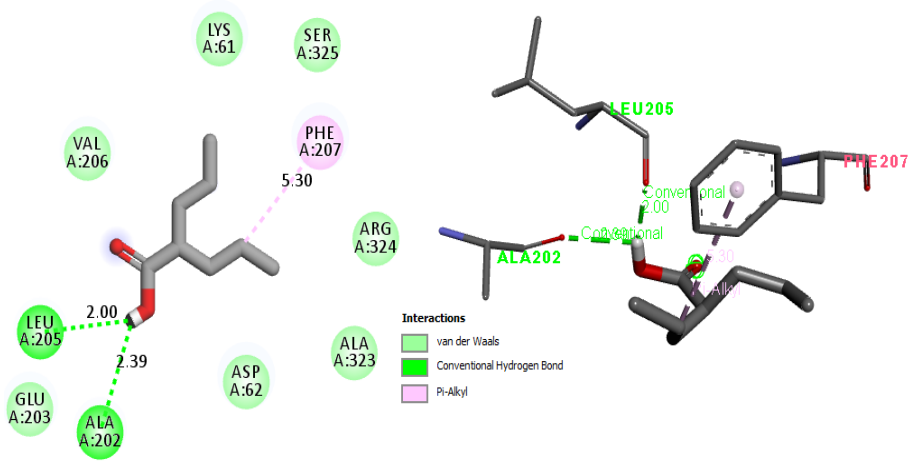

Figure 10. 2D and 3D representation of valproic acid and 4KFM macromolecule

The resulting ligand-protein interactions are the; 2.27Å interaction long hydrogen bond interaction with the LEU_A273 amino acid active site amine group; the VAL_A235 amino acid active site formed a 3.86Å long alkyl bond interaction with the methylene group (Table 8).

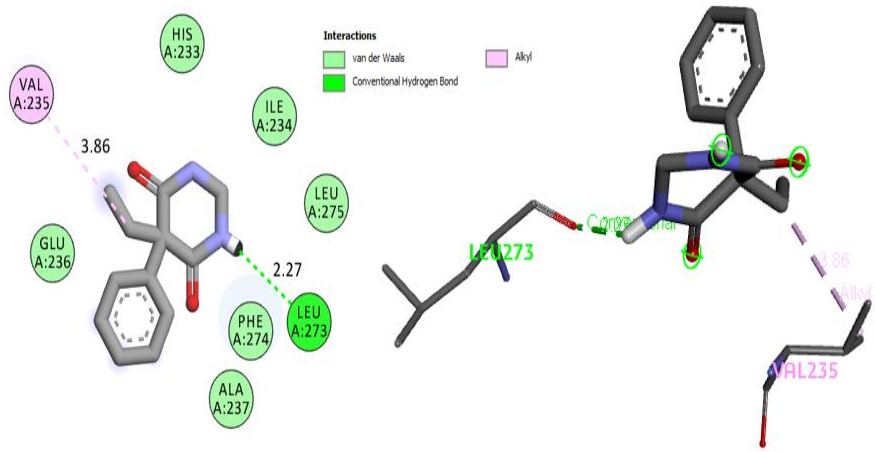

Figure 11. 2D and 3D representation of primidone and 4KFM macromolecule

3.12. Remasemid

The affinity value of remasemide placed in 4KFM at the best binding position was obtained as -5.9 kcal/mol. 2D and 3D shapes of interactions between remasemid and 4KFM are presented in the fig. 12 and interactions after molecular docking are the; PHE_A83 and PHE_A186 amino acid active sites interacted with benzene group of 3.83Å and 3.70Å length pi-pi stacked bond, respectively (Table 8).

Table 8. Interactions, types and distances between primidone and remasemid and the 4KFM macromolecule

Primidone				Remasemid			
Residue	**Ligand group**	**Distance (Å)**	**Interaction**	**Residue**	**Ligand group**	**Distance (Å)**	**Interaction**
LEU_A273	NH_2 compound in primidone	2,27	Carbon hydrogen bond	PHE_A83	Benzene group in remasemid	3,83	Pi-Pi Stacked
VAL_A235	CH_2 compound in primidone	3,86	Alki-yl	PHE_A186	Benzene group in remasemid	3,70	Pi-Pi Stacked

The interactions found for primidone and remasemid are shown in Table 8.

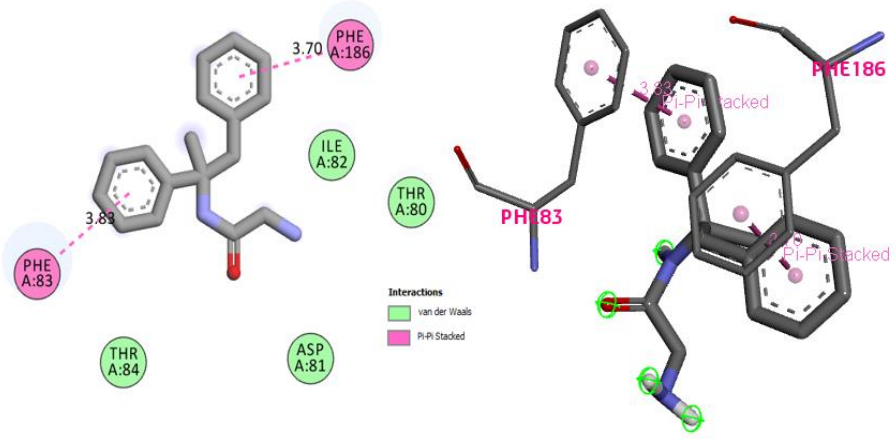

Figure 12. 2D and 3D representation of remasemid and 4KFM macromolecule

3.13. Phenytoin

The affinity value of phenytoin at the best binding position was -6.2 kcal/mol. Pictures of interactions between phenytoin and 4KFM are presented in the fig. 13 and post-study interactions are the; conventional hydrogen bond interaction with the amine group of the amino acid active site of ARG_A57 with a length of 1.99Å; LEU_A257 and LEU_B53 amino acid active sites formed pi-sigma and pi-alkyl bond interactions with benzene group of 3.62Å and 5.18Å, respectively (Table 9).

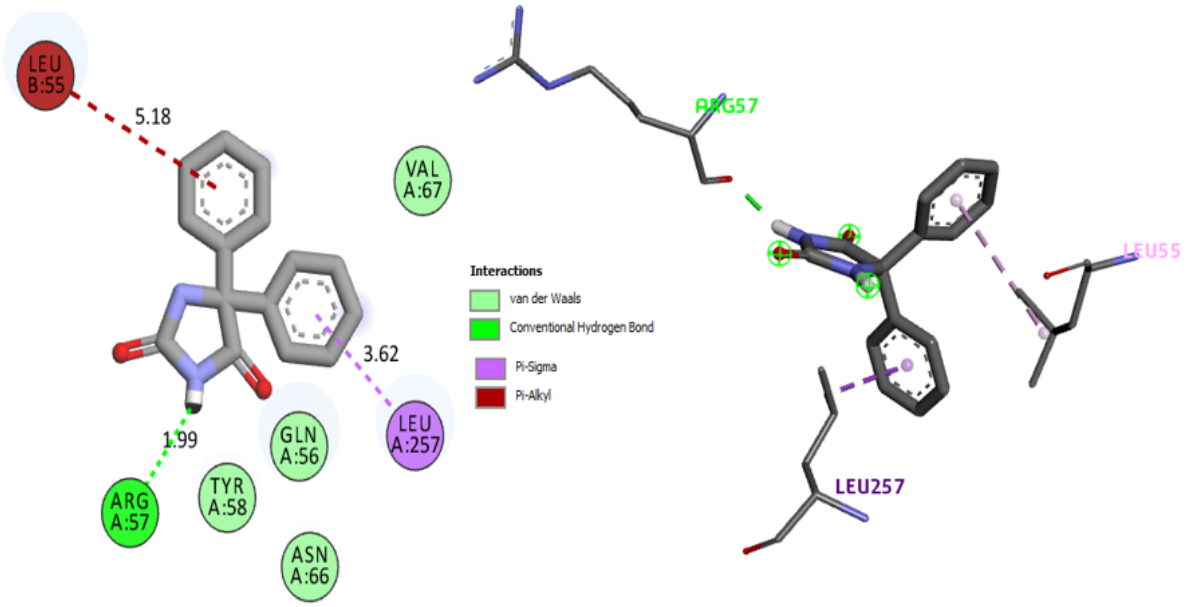

Figure 13. 2D and 3D representation of phenytoin and 4KFM macromolecule

3.14. Ethotoin

The affinity value of the ethhotoin placed in the macromolecule 4KFM at the best binding position was obtained as -5.5 kcal/mol and pictures of the interactions between the ethotoin and 4KFM are shown in the fig. 14. The interactions obtained are the; conventional hydrogen bond interaction of PHE_A207 amino acid active site with amine group of 2.90Å length; 3.38Å length carbon hydrogen

bond interaction with O atom of LYS_A61 amino acid active site; the LYS_A61 amino acid active site formed a 3,76Å long alkyl bond interaction with the methylene group (Table 9).)

Table 9. Interactions, types and distances between phenytoin and ethotoin and 4KFM macromolecule

Fenitoin				Ethotoin			
Residue	**Ligand group**	**Distance (Å)**	**Interaction**	**Residue**	**Ligand group**	**Distance (Å)**	**Interaction**
ARG_A57	NH_2 compound in phenytoin	1,99	Conventional hydrogen bond	PHE_A207	NH_2 compound in ethotoin	2,90	Conventional hydrogen bond
LEU_A257	Benzene group in phenytoin	3,62	Pi-Sigma	LYS_A61	O atom in ethhotoin	3,38	Carbon hydrogen bond
LEU_B53	Benzene group in phenytoin	5,18	Pi-Alkyl	LYS_A61	CH_2 compound in ethotoin	3,76	Alkyl

The interactions found for fenitoin and ethotoin are shown in table 9.

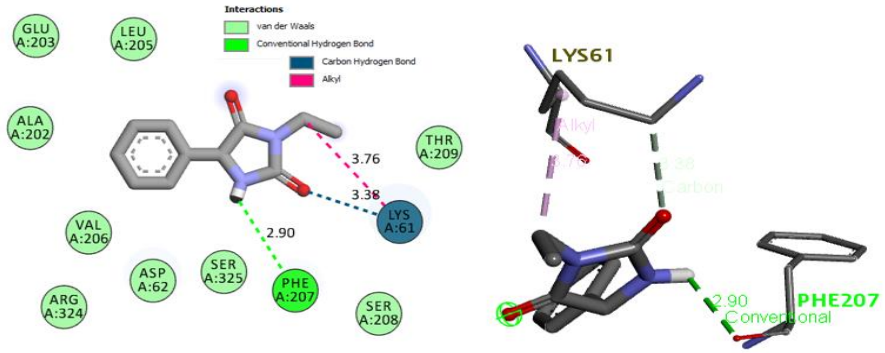

Fig. 14. 2D and 3D representation of ethotoin and 4KFM macromolecule

3.15. Trimethadion

The affinity value of trimethadione at the best binding position was achieved as -4.7 kcal/mol, and 2D and 3D shapes of intermolecular interactions between trimethadione and macromolecule are shown in the fig. 15. Interactions are the; the amino acid binding sites ARG_A324, ALA_A323, ALA_A202, ALA_A202, LYS_A64 and LYS_A199 were respectively 3,64Å with methyl group; 3.95Å; 3.47Å; 4.08Å; they formed the interaction of carbon hydrogen bond, alkyl, alkyl, alkyl, alkyl and alkyl bonds, respectively, 4.54Å and 4.31Å in length (Table 10).

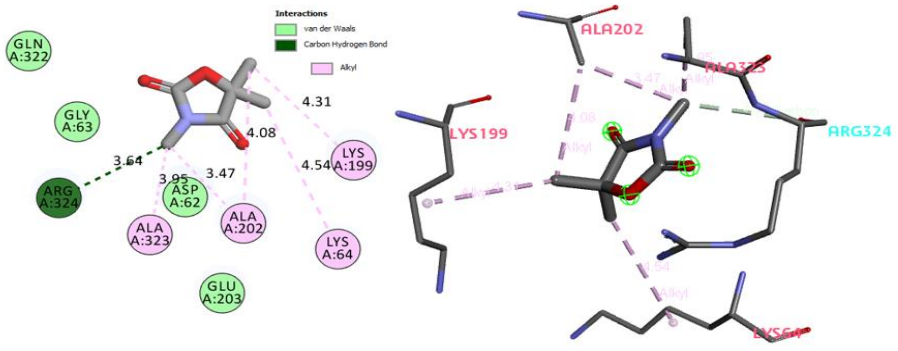

Figure 15. 2D and 3D representation of trimethadion and 4KFM macromolecule

3.16. Levetiracetam

The affinity value of levetiresetam at the best binding position was obtained as -4.5 kcal/mol, and pictures of the molecular interactions between levetiresetam best binding position and 4KFM are shown in the fig. 16. The resulting ligand-protein interactions were as follows; the amino acid binding sites ALA_A202, GLU_A203 and LEU_A205 with the amine group were 2.59Å length, respectively; conventional hydrogen bond interaction of 2.38Å and 2.31Å length; the amino acid active sites LEU_A205, ALA_A323 and PHE_A207 were 3.75Å length with methylene group; carbon hydrogen bond, alkyl and pi-alkyl bond interaction, respectively, at 4.40Å and 5.46Å length; 3.78A length long carbon hydrogen bond interaction with GLU_A203 amino acid active site O atom; the ASP_A62 amino acid binding site formed a 3,55Å long carbon-hydrogen bond interaction with the carbon atom (Table 10).

Table 10. Interactions their types and distances between levetiresetam and trimethadion and 4KFM macromolecule

Levetiresetam				Trimethadion			
Residue	**Ligand group**	**Distance (Å)**	**Interaction**	**Residue**	**Ligand group**	**Distance (Å)**	**Interaction**
ALA_A202	NH_2 compound in levetiresetam	2,59	Conventional hydrogen bond	ARG_A324	CH_3 compound in trimethadion	3,64	Carbon hydrogen bond
GLU_A203	NH_2 compound in levetiresetam	2,38	Conventional hydrogen bond	ALA_A323	CH_3 compound in trimethadion	3,95	Alkyl
LEU_A205	NH_2 compound in levetiresetam	2,31	Conventional hydrogen bond	ALA_A202	CH_3 compound in trimethadion	3,47	Alkyl
GLU_A203	O atom in levetiracetam	3,78	Carbon hydrogen bond	ALA_A202	CH_3 compound in trimethadion	4,08	Alkyl
LEU_A205	The methylene group in levetircetam	3,75	Carbon hydrogen bond	LYS_A64	CH_3 compound in trimethadion	4,54	Alkyl
ALA_A323	The methylene group in levetircetam	4,40	Alkyl	LYS_A199	CH_3 compound in trimethadion	4,31	Alkyl
PHE_A207	The methylene group in levetircetam	5,46	Pi- Alkyl				
ASP_A62	C atom in levetircetam	3,55	Carbon hydrogen bond				

The interactions found for levetiresetam and trimethadion are shown in table 10.

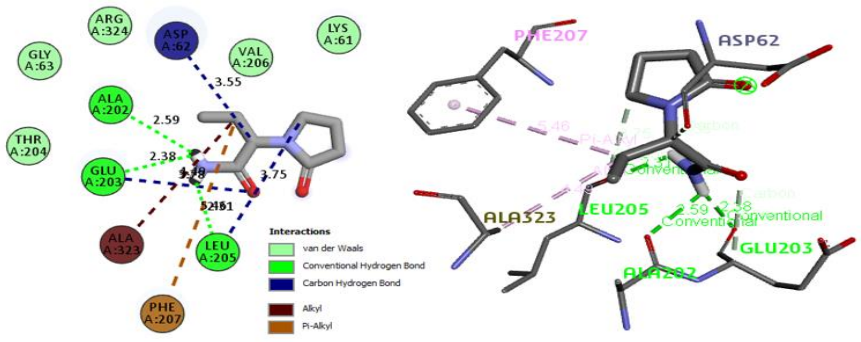

Figure 16. 2D and 3D representation of levetiresetam and 4KFM macromolecule

3.17. Topiramate

The affinity value of topiramate at the best binding position was obtained as -5.8 kcal/mol, and 2D and 3D pictures of the interactions of molecules with 4KFM are presented in the fig. 17. The interactions obtained are as follows; 3.48Å long carbon hydrogen bond interaction with LEU_A205 amino acid active site C atom; pi-donor hydrogen bond interaction with HIS_A357 amino acid binding site amine group, respectively, 3.08Å long; the LYS_A61 amino acid active site formed an alkyl bond interaction with the methyl group of 4.11Å and 4.09Å, respectively (Table 11).

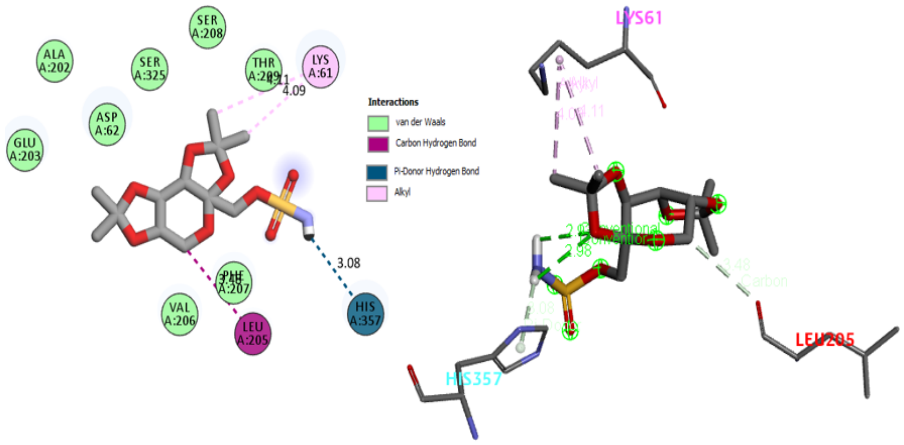

Figure 17. 2D and 3D representation of topiramate and 4KFM macromolecule

3.18. Mesuximide

The mesuximide binding affinity value was obtained as -5.7 kcal/mol, and the patterns of molecular interactions between the best binding mode and 4KFM are presented in the fig. 18 and the interactions were as follows; ALA_A323 and ALA_A202 amino acid active sites with benzene group 5,31Å and 3,83Å long pi-alkyl and amide-pi stacked bond interaction, respectively; the VAL_A206 and LYS_A61 amino acid active sites formed an alkyl bond interaction with the methyl group of 4.82Å and 4.96Å long, respectively (Table 11).

Table 11. Interactions, types and distances between topiramate and mesuximide and the 4KFM macromolecule

Topiramat				Mesuximide			
Residue	**Ligand group**	**Distance (Å)**	**Interaction**	**Residue**	**Ligand group**	**Distance (Å)**	**Interaction**
LEU_A205	C atom in topiramate	3,48	Carbon hydrogen bond	ALA_A323	Benzene group in mesuximide	5,31	Pi- Alkyl
HIS_A357	NH_2 group in topiramate	3,08	Pi-donor hydrogen bond	ALA_A202	Benzene group in mesuximide	3,83	Amid-Pi Stacked
LYS_A61	The methyl group in topiramate	4,11	Alkyl	VAL_A206	CH_3 group in mesuximide	4,82	Alkyl
LYS_S61	The methyl group in topiramate	4,09	Alkyl	LYS_A61	CH_3 group in mesuximide	4,96	Alkyl
LEU_A205	C atom in topiramate	3,48	Carbon hydrogen bond				

The interactions found for topiramat and mesuximide are shown in Table 11.

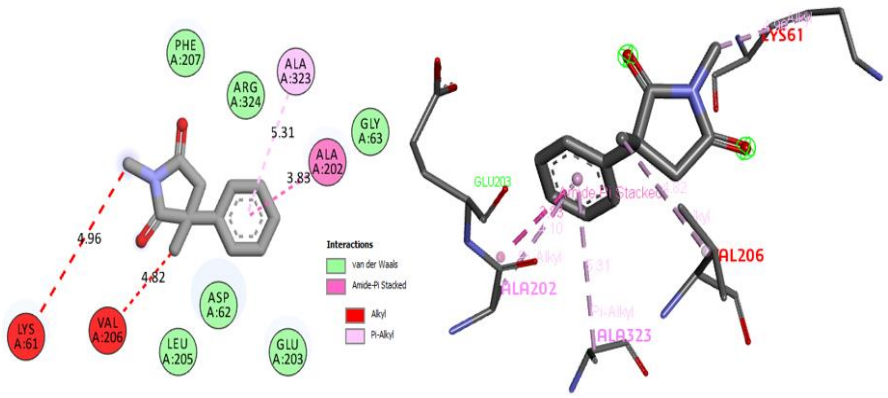

Figure 18. 2D and 3D representation of mesuximide and 4KFM macromolecule

3.19. Mephenytoin

The binding affinity value of mephenytoin at the best binding position was achieved as -5.5 kcal/mol, and the patterns of molecules interactions between the best binding position and 4KFM are shown in the fig. 19. Ligand-protein interactions are the; HIS_A357 amino acid binding site formed 4,59Å long, pi-alkyl interaction with the methyl group (Table 12).

Table 12. Communications, species and distances between mephenytoin and 4KFM macromole

Mephenytoin			
Residue	**Ligand group**	**Distance (Å)**	**Interaction**
HIS_A357	CH_3 compound in mephenytoin	4,59	Pi-Alkyl

The interactions found for mephenytoin are shown in table 12.

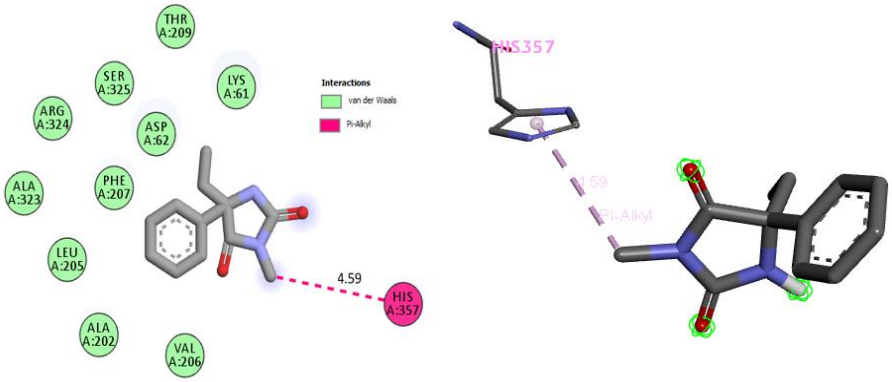

Figure 19. 2D and 3D representation of mephenytoin and 4KFM macromolecule

4. Conclusions

Only DOCK energy scoring was used in the study, but there are also various scoring functions. The results show that the 4KFM coded macromolecule can best achieve its potency for potassium channels, which has an important impact on its role in epilepsy treatment, with phenytoin. Another piece of information provided by the docking study is that the conventional hydrogen bonding and carbon-hydrogen bond formation between the receptor and the ligands create a strong bond, and the

appearance of these bonds can have a good effect on the resulting complex structure. Therefore, structures that form strong bonds give better results than others. Piplani et al. (2016) found that the data they obtained for the antiepileptic drug active ingredients we examined in their implantation study with PDB ID: 1Q55 were more or less similar to the results we found. In both studies compared, valproic acid gave the lowest interaction compared to the others [18]. In another study, Gilani et al. (2019) found the affinity value of -2.803 kcal/mol as a result of a vigabatrin coupling study with the 1HOV macromolecule, but here the 4KFM macromolecule gave a better affinity value for vigabatrin [19]. For zonisamide, Shahabadi et al. (2013) found a value of -6.86 kcal/mol in their coupling study with the 1AO6 macromolecule, a result of -5.5 kcal/mol was found when compared with the 4KFM macromolecule. It can be said that the binding affinity of the 1OA6 macromolecule on zonisamide is better [20] . Tripathi and Ayyanna (2017) found 5.34 kcal/mol and -6.68 kcal/mol values for phenytoin and lamotrigine in coupling study with 2KAV macromolecule, respectively, while comparing the binding affinity values found for the complex structure of 4KFM-phenytoin and 4KFM-lamotrigine[21]. The interaction of 4KFM-phenytoin structure occurs the strongest, while weak results were obtained for 4KFM-lamotrigine. Fijalowski et al. (2017) conducted a molecular docking study between the active ingredients of gabapentin, lamotrigine, tiagabine, valproic acid, zonisamide and vigabatrin and the hGAT1 macromolecule. Compared to the molecular coupling process with 4KFM, 4KFM gave higher affinity value for active ingredients other than valproic acid, tiagabine and vigabatrin. The discussed data show that AEDs are frequently used materials in molecular docking studies [22]. And, according to the docking results compared with other studies, it has been seen that affinity values may be close to each other. If we compare the data obtained as a result of molecular coupling of the ligands with the PDB ID file 4KFM, which was studied as a K^+ channel agonist, the highest binding affinities were -6.2 kcal/mol the 4KFM-phenytoin complex structure.

Table 13. Comparison of bond and energy in ligand-4KFM structure

Conventional Hydrogen Bonding Ligands	Number Of Ties	Binding Energy (kcal/mol)
Vigabatrin	3	-4,0
Locosamidine	1	-5,0
Zonisamide	2	-5,5
Oxcarbazepine	0	-6,0
Levetiracetam	3	-4,5
Tiagabine	0	-5,7
Topiramate	0	-5,8
Lamotrigine	0	-5,6
Gabapentin	0	-4,8
Felbamate	4	-5,7
Ethosuximide	2	-4,6
Valproic Acid	0	-3,9
Mesuximide	0	-5,7
Ethotoin	1	-5,5
Primidone	0	-5,8
Trimethadione	0	-4,7
Phenytoin	1	-6,2
Remasemide	0	-5,9
Mephenytoine	0	-5,5

Then oxcarbezepine with a value of -6.0 kcal/mol; Remasemide with -5.9 kcal/mol; Primidone and topiramate structures come with -5.8 kcal/mol. These substances were followed by tiagabine, felbamate and mesuximide with -5.7 kcal/mol; Lamotrigine with a value of -5.6 kcal/mol; Zonisamide, ethotoin and mephenytoin with -5.5 kcal/mol; Locosamide with -5.0 kcal/mol; Gabapentin with -4.8 kcal/mol; Trimethadione with -4.7 kcal/mol; Ethosuximide with -4.6 kcal/mol;

Levetiresetam with -4.5 kcal/mol; Vigabatrin with -4.0 kcal/mol and valproic acid complex structures with -3.9 kcal/mol. As a result, when looking at the data, it is seen that it is the active substance phenytoin that acts best as a potassium channel agonist.

Looking at table 13, it is seen in which antiepileptics the traditional hydrogen bond formed between the studied ligands and 4KFM and the number of bonds. Despite the conventional hydrogen bonding, the bonding energy of the structure was compared. It is seen that; Although phenytoin gave the best binding energy, it was able to make one of the desired conventional hydrogen bonds. Oxcarbazepine, which gave the best binding energy immediately after, could not form any conventional hydrogen bonds. It is seen that felbamate has made 4 conventional hydrogen bonds, but it is seen that this desired bond cannot be obtained in ligands with better binding energy. Although vigabatrin, ethosuximide and levetiracetam gave the lowest bond energies, it was observed that they formed 3, 2 and 3 conventional hydrogen bonds, respectively. It is seen that only 8 ligands (green color) out of 19 structures form this bond, while 8 structures (orange color) with good binding energy do not. It was observed that the remaining 3 structures (gri color) with low binding energy did not give conventional hydrogen bonding.
It can be concluded that there is no direct proportionality between the best binding energy obtained and the bond structures formed.

Authors' Contributions

ENÇ and MG designed the structure. MG determined the suitability selection of materials. ENÇ ran the program, did his studies, theoretical calculations and wrote the article. MG and BK are the overall supervisors of the project.

Both authors read and approved the final manuscript.

Competing Interests

The authors declare that they have no competing interests.

References

[1]. W. Loscher, "Current status and future directions in the pharmacotherapy of epilepsy," *Trends Pharmacol Science,* vol. 23, no. 3, pp. 113-118, 2002.
[2]. A. K. Ngugi, S. M. Kariuki, C. Bottomley, I. Kleinschmidt, J. W. Sander, and C.R. Newton, "Incidence of epilepsy: a systematic review and meta-analysis," *Neurology,* vol. 77, no. 10, pp. 1005-1012, 2011.
[3]. H. E. Scharfman, "The neurobiology of epilepsy," *Current Neurology and Neuroscience Reports,* 7(4):348-354, 2007.
[4]. J. Q. Kang, and R. L. Macdonald, "Making sense of nonsense GABA(A) receptor mutations associated with genetic epilepsies," *Trends in Moleculer Medicine,* vol. 15, no. 9, pp. 430-438, 2009.
[5]. R. Wallace, "Mutations in GABA-receptor genes cause human epilepsy," *The Lancet Neurology*, vo. 1, no. 4, pp. 212, 2002.
[6]. G. Krapivinsky, E. A. Gordon, K. Wickman, B. Velimirovic, L. Krapivinsky, and D. E. Clapham, "The Gprotein-gated atrial K+ channel IKACh is a heteromultimer of two inwardly rectifying K(+)-channel proteins," *Nature,* vol. 374, no. 6518, pp. 135-141, 1995.
[7]. P. A. Slesinger, E. Reuveny, Y. N. Jan, and L. Y. Jan, "Identification of structural elements involved in G protein gating of the GIRK1 potassium channel," *Neuron,* vol. 15, no. 5, pp. 1145-1156, 1995.

[8]. E. Akyüz, and P. M. Tiber, "İçeri doğrultucu potasyum kanalları ve epilepsi", *Journal of Harran University Medical Faculty*, vol. 14, no. 2, pp. 141-149, 2017.
[9]. P. R. Camfield, C. S. Camfield, K. F. Swaiman, S. Ashwal, and D. M. Ferriero, "Pediatric Epilepsy: Pediatric Neurology Principles & Practice," *Mosby Elsevier*, vol. 1, no. 9996004716, pp. 981-989, 2006.
[10]. C. L. Deckers, P. Genton, G. J. Sills, and D. Schmidt, "Current limitations of antiepileptic drug therapy: a conference review," *Epilepsy Research*, vol. 53, pp. 1-17, 2003.
[11]. C. A. Doupnik, "Identification of aethina tumida kir channels as putative targets of the bee venom peptide tertiapin using structure-based virtual screening methods," *Toxins*, vol. 11, no. 546, pp. 1-17, 2009.
[12]. Y. Zhao, P. Man-UnUng, G. Zahora´nszky-Kohalmi, A. Schlessinger, J. J. Marugan, and P. A. Slesinger, "Identification of a G-protein-ındependent activator of gırk channels," *Cell Reports*, vol. 31, no. 11, pp. 1-18, 2020.
[13]. https://www.rcsb.org/structure/4kfm Date of access 20. 12, 2022.
[14]. M. R. Whorton, and R. Mackinnon, "X-ray structure of the mammalian GIRK2-beta gamma G-protein complex," *Nature*, vol. 498, no. 7453, pp. 190-197, 2013.
[15]. Dassault Systèmes BIOVIA, Discovery Studio Modeling Environment, Release 2017, San Diego: Dassault Systèmes, 2016.
[16]. J. Eberhardt, D. Santos-Martins, A. F. Tillack, and S. Forli, "AutoDock Vina 1.2.0: New Docking Methods, Expanded Force Field, and Python Bindings," *Journal of Chemical Information and Modeling*, 2021.
[17]. O. Trott, and A. J. Olson, "AutoDock Vina: improving the speed and accuracy of docking with a new scoring function, efficient optimization and multithreading," *Journal of Computational Chemistry*, vol. 31, pp. 455-461,2010.
[18]. S. Piplani, V. K. Saini, R. R. Niraj, A. Pushp, and A. Kumar, "Homology Modlling and molecular kenetleme studies of human placental cadherin protein for its role in teratogenic effects of anti-epileptic drugs," *Computational Biology and Chemistry*, vol. 60, pp. 1-8, 2016.
[19]. S. Jamal Gilani, M. Zaheen Hassan, S. Sarim Imam, C. Kala, and S. P. Dixit, "Novel benzothiazole hydrazine carboxamide hybrid scaffolds as potential in vitro GABA-AT enzyme inhibitors: Synthesis, molecular kenetleme and antiepileptic evaluation," *Direct Bioorganic & Medicinal Chemistry Letters*, vol. 29, pp. 1825-2830, 2019.
[20]. N. Shahabadi, A. Khorshidi, and N. M. Moghadam, "Study on the Etkileşim of the epilepsy drug, zonisamide with human serum albumin (HSA) by spectroscopic and molecular docking techniques," *Spectrochimica Acta Part A: Molecular and Biomolecular Spectroscopy*, vol. 114, pp. 627-632, 2013.
[21]. R. K. Prasad Tripathi, and S. R. Ayyannan, "Anticonvulsant activity, organotypic hippocampal neuroprotection assay and in-silico sodium channel blocking potential of 2-amino-6nitrobenzothiazole derived semicarbazones," *Biomedicine & Pharmacotherapy*, vol. 95, pp. 1451-1460, 2017.
[22]. L. Fijalkowski, K. Salat, A. Podkowa, P. Zaręba, and A. Nowaczyk, "Potential role of selected antiepileptics used in neuropathic pain as human GABA transporter isoform 1 (GAT1) inhibitors-Molecular docking and pharmacodynamic studies," *European Journal of Pharmaceutical Sciences*, vol. 96, pp. 362-372, 2017.